Optimization of ranitidine hydrochloride removal from simulated pharmaceutical waste by activated charcoal from mung bean husk using response surface methodology and artificial neural network

Sandip Mondal[a,b], Kaustav Aikat[a], Gopinath Halder[b,*]

[a]*Department of Biotechnology, National Institute of Technology Durgapur, M.G. Avenue, Durgapur, West Bengal 713209, India,*
Tel. +91 81015 83685; email: mondal.sandip4@gmail.com (S. Mondal), Tel. +91 94347 88140; email: aikatk@yahoo.co.in (K. Aikat)
[b]*Chemical Engineering Department, National Institute of Technology Durgapur, M.G. Avenue, Durgapur, West Bengal 713209,*
India, Tel. +91 94347 88189; Fax: +91 343 2547375/2546735; emails: gopinathhaldar@gmail.com, gopinath_haldar@yahoo.co.in

ABSTRACT

The removal of ranitidine hydrochloride (RH) from simulated pharmaceutical aqueous solution using steam-activated charcoal from mung bean husk (MBH) by batch adsorption technique was investigated. The adsorbent was characterized by Brunauer–Emmett–Teller surface area analyzer, SEM, and point of zero charge. The influence of three process parameters such as adsorbent dose, solution pH, and agitation on the performance of the activated carbon was studied. The removal of 100 mg L^{-1} RH was 99.16% at pH 2, adsorbent dose 0.75 gm L^{-1}, and agitation speed of 180 rpm. The effects of process parameters on the removal efficiency were optimized as per central composite design of response surface methodology (RSM), and the same design was used for training set for artificial neural network (ANN). The results showed that ANN has better prediction capability as compared to RSM and SAC developed from MBH could be a promising adsorbent for RH removal from simulated pharmaceutical waste.

Keywords: Ranitidine hydrochloride; Mung bean husk; Simulated pharmaceutical waste; Response surface methodology; Artificial neural network

1. Introduction

In the last century, the presence of micro-pollutant like pharmaceutical compound (PC) in the environment has raised a serious concern among researchers, regulatory agencies, and plant manufacturer due to their subtle detrimental effects on aquatic systems and possible unknown effect on human health at a very low concentration [1–7]. The intrinsic properties such as high polarity and persistence make PC to reach and accumulate in water bodies. Generally, municipal wastewater treatment plants are not well equipped to remove this complex compound [8–13]. Ranitidine hydrochloride (RH), a histamine H_2-receptor antagonist, is one of the world's largest selling drugs. RH may enter the environment from excretion by patients, pharmaceutical waste disposal, and emission from manufacturing sites. RH has LC_{50} value higher than 100 mg L^{-1} which is classified as not being harmful to aquatic organisms according to EU-Directive 93/67/EEC (Commission of the European Communities, 1996). But recent studies of Isidori et al. found that the

*Corresponding author.

photo-degraded product of ranitidine was potentially hazardous in the order of tenths of mg per liter [14].

Several methods have been employed to remove pharmaceuticals from the environment and this includes oxidation and ozonation [15–17], photo degradation [18], adsorption, [19,20], photo-Fenton degradation [21], coagulation–flocculation [22], reverse osmosis [23], chlorination [24], and photo catalytic oxidation [25]. Among these methods, adsorption process seems to be an attractive solution of pharmaceutical removal due to its convenience, effectiveness, and economical property [26]. Till now, removal of PC has been achieved using activated carbon [27–29], zeolites [30,31], carbon nanomaterial's [32], minerals [33], hybrid particle [34,35], inorganic–organic-modified bentonite [36,37], mesoporous silica based material [38], etc. Of these several adsorbents, activated carbon has a high specific surface area, fast adsorption kinetics so thus adsorbs a wide range of organic and inorganic pollutants from aqueous solution. However, despite so many advantages, the use of commercially activated carbon is very costly due to nonrenewable and relatively expensive starting material such as coal, which is not justified for pollution control [39]. Therefore, the researchers paid attention to the preparation of activated carbon from low cost precursor such as agrowaste material. In the present investigation, mung bean husk (MBH) has been converted into activated carbon and it is used for the removal of RH under the influence of different parameters. Mung bean, the seeds of *Vigna radiate*, is native from the Indian subcontinent and it is one of the most important grain legumes in South Asia [40]. The large amount of husk, an agro by-product that is produced during milling of mung bean by legume seed splitting process, has been used as an adsorbent for RH removal.

In recent years, multivariate statistical tools (MST) have been used to reduce the cost and time of an experiment. This multivariate statistical method also helped to identify the optimal condition of factors and interaction among factors that are not possible using the only univariate method [41]. The experimental design estimates the coefficient in a mathematical model that predicts the response and checks the suitability of the method. Of different MST, response surface methodology (RSM) and artificial neural network (ANN) have been used for modeling and optimizing the process parameters. These two tools are compared to check the superiority over other and to understand the process under investigation as well.

RSM is a statistical tool for modeling and analysis of a problem where a response of interest is influenced by several parameters [42]. A central composite design (CCD) is a tool of standard RSM design which has been applied in this work for modeling and optimization of RH removal. RSM is a quadratic surface fitting tool for the optimization of effective variables (dose, pH and agitation) with a minimum number of experiments and it helps to analyze the interaction between the parameters [43]. In general, the CCD is a 2^n factorial run with $2n$ axial runs and n_c center runs.

ANN is an artificial intelligence system based on the structure of a biological neural system for solving problems. It is a very powerful technique which can make a decision and draw conclusions in the case of complex, noisy, and partial information. In the present investigation, the experimental system is modeled and optimized by ANN system. Numerous application of ANN has been conducted to solve environmental problems due to its reliability and robustness in capturing the nonlinear relationships existing between variables in a complex system.

In this study, a two level-three factors (2^3) full factorial CCD in RSM and ANN model system have been developed to predict the relationship between the experimental variables (dose, pH, and agitation) and response variable (removal rate of RH). Finally, the batch-optimized results have been evaluated statistically in terms of coefficient of determination (R^2), root-mean-square error (RMSE), and absolute average deviation (AAD) based on the validation data-set.
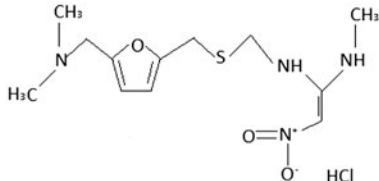
2. Materials and methods

All chemicals used in this study were of analytical reagent grade. The RH was purchased from Sigma-Aldrich, India. The physicochemical properties of RH are depicted in Table 1. Drug solution was prepared from doubly distilled water by Merck Millipore water system (Merck, Germany).

2.1. Preparation of activated carbon from mung husk

The raw material of activated carbon, the MBH, was obtained from a local shop in Durgapur, India. The MBH was washed with bi-distilled water for several times and dried them in hot air oven to obtain the preferred precursor. The raw material was carbonized gradually (rate of 55°C/15 min) at 550°C for 1 h in a stainless steel sphere-shaped furnace chamber. In the next step, the temperature was raised to 650°C and superheated steam was introduced into the furnace chamber for 1 h for activation of carbonized

Table 1
Some physicochemical properties of RH

Generic name	Structure	Molecular mass (g mol^{-1})	pK_a	log K_{0w}
Ranitidine hydrochloride		350.87	8.2 and 2.7	0.27

char. The activated carbon product was then cooled to room temperature and used for the experiment.

2.2. Preparation of adsorbate solutions

RH (C$_{13}$H$_{22}$N$_4$O$_3$S·HCl, M.W. 350.87) was purchased from Sigma-Aldrich in commercial quality grade. A stock solution of 400 mg L^{-1} was prepared by dissolving accurately weighed out quantity of RH in doubly distilled water. The solution of pH was adjusted using 0.1 N NaOH and 0.1 N HCl.

2.3. Batch mode adsorption studies

The adsorption of RH onto MHAC was measured by the batch equilibrium study. All batch experiments were preformed in 100 ml of working volume of liquid sample with a concentration of 100 mg L^{-1} of RH. Optimum condition of dose, pH, and rpm was determined in an incubator shaker (Model Innova 42, New Brunswick Scientific, Canada) at 310 K. This study was conducted in a variable dose (75 mg^{-1} gm), pH (2–10), and rpm (40–240) for a predetermined contact time interval (up to 180 min). Samples were taken from the flask at a specified time interval to analyze the drug concentration in the solution. The remaining amount of drug was investigated in each flask using UV–vis spectrophotometer (Model Hitachi-2800, Japan). All batch experiments were carried out in triplicate, and the mean values were used in the data analysis. The amount of PC adsorbed at equilibrium q_e (mg g^{-1}) can be calculated from the initial and final equilibrium concentrations according to the mass balance using the following equation:

$$q_e = \frac{(C_i - C_e)V}{m} \qquad (1)$$

where C_i is the initial pharmaceutical concentration, mg L^{-1} and C_e is the equilibrium pharmaceutical concentration, mg L^{-1}.

The percent removal of RH was calculated using the following relation:

$$\text{Sorption } (\%) = \frac{(C_i - C_e)}{C_i} \times 100 \qquad (2)$$

Control experiments were also performed to verify that no sorption effect of RH was on the wall of the flask.

2.4. Experimental design

2.4.1. Optimization of adsorption methods by RSM

The optimization of RH removal was carried out through RSM by three independent chosen process variables, namely adsorbent dose, pH, and agitation. The concentration of RH used in RSM was 100 mg L^{-1}. A CCD was selected for the experimental design of RSM to develop a quadratic model for describing the drug removal process. The ranges and levels of variables used in this study are given in Table 2. The percent removal of the drug was taken as the response of the system.

The correlation between response function and process variables can be expressed by a quadratic equation [44] that is given as:

$$x_j \gamma = \beta_0 + \sum_{i=1}^{k} \beta_i x_i + \sum_{i=1}^{k} \beta_{ii} x_i^2 + \sum_{i=1} \sum_{j=1+1} \beta_{ij} x_i x_j + \varepsilon \qquad (3)$$

where β_0 is the constant coefficient, β_i, β_{ii} and β_{ij} is the coefficients for the linear, quadratic, and interaction effect, respectively, x_i, x_j is the independent variables and ε is the error.

In CCD, the generation of response surface contour plot helps to study the interaction between the different independent variables and their corresponding effect.

Table 2
Experimental range and levels of independent process variables used as per CCD

Variable	Unit	Range and levels (coded values)				
		$-\alpha$	-1	0	$+1$	$+\alpha$
Adsorbent dose (A)	mg	77.28	350	750	1,150	1,422.72
pH (B)		1.95	4	7	10	12.05
Agitation speed (C)	rpm	45.91	80	130	180	214.09

2.4.2. Optimization of the adsorption method by ANN structure

ANN model processes the data and makes an optimal decision by the way the biological nervous system does. There are several kinds of ANN models developed such as multilayer perception, feed forward, and radial basis function etc. for engineering application. In this study, a three layer feed forward, back propagation neural network with a linear transfer function was developed for modeling of RH removal from simulated water.

Basically, ANN consists of three layers: input layer, a number of hidden layers, and an outer layer. Input and hidden layer are independent variable where the outer layer is a dependent variable. The architecture of ANN model is such that these three layers are well connected via interconnected processing unit called neuron, and each neuron is connected to another neuron via links. External source feed in information to the input layer which in turn passes the information to the hidden layer for data processing. Each of the input values was weighted individually before entering into the hidden layer. The hidden layer analyzes all the data processing, and according to the sum of the weighted values from input layer, it produces the output [45].

In this study, the input to ANN model was same as that of RSM model, viz. adsorbent dose, pH, and agitation. The input and output prototype required for training were obtained from adsorption experimentation through CCD. All of the calculations of ANN were carried out using a neural network toolbox of MATLAB version 7.12.

3. Results and discussion

3.1. Characterization of activated carbon

The characteristics of activated charcoal are very important factor to understand the adsorption mechanism and fate of micro-pollutant. The Brunauer–Emmett–Teller (BET) method was used to measure specific surface area, total pore volume, and pore size distribution of the prepared activated carbon at 77 K by means of N_2 adsorption [46]. Scanning electron microscopy (SEM) analysis was carried out to investigate the surface textures and the development of pore of sorbent material. Furthermore to know the surface chemistry of the adsorbent, pH of the point of zero charge (pH_{pzc}) of adsorbent was also measured [47]. In Table 3, the physicochemical properties of MBH-based activated carbon are presented.

In our previous study [48], the characterization of activated charcoal derived from MBH have been described in detail. In this study, some of those parameters has been explained briefly only for data interpretation purposes.

BET surface area and pore volume of the adsorbent material was found to be 405 $m^2 g^{-1}$ and 0.29 $cm^3 g^{-1}$ by applying BET equation from N_2 adsorption. The activated charcoal surface structure was found to be porous, irregular shaped, and uneven in SEM micrograph as shown in Fig. 1(a). High heterogeneous porous structure is associated with high surface area. In Fig. 1(b), it was seen that the number of pore structure was reduced and it helped to entrap the drug molecule inside the surface of the activated charcoal thus helps absorption. The pH of the point of zero charge of adsorbent was found to be 8.6 that indicate the "H" type carbon. H type carbons (lower density of oxygen-containing function group) are more hydrophobic and possess strong adsorption capacity.

Table 3
Some physicochemical properties of the activated carbon prepared from MBH

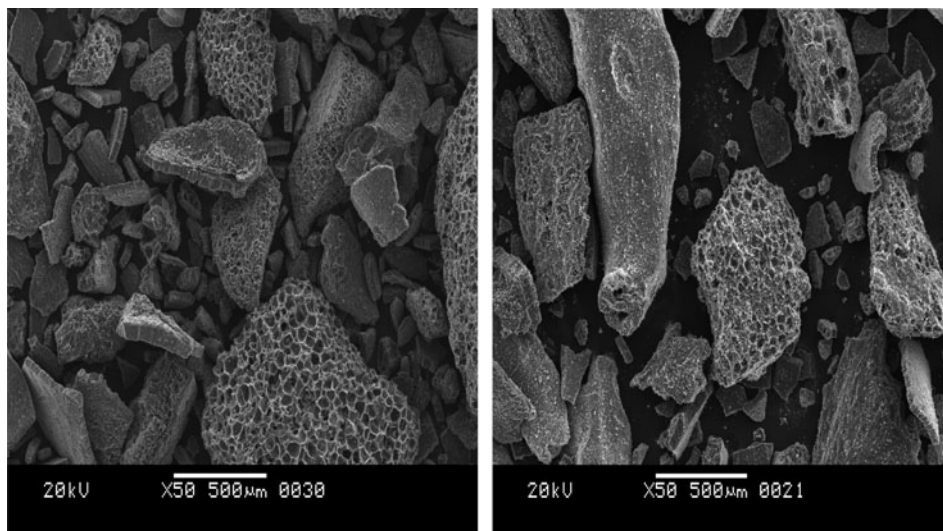| SI no.	Properties	Value
1	Volatile matter	7.681%
2	Moisture	0.722%
3	Ash content	8.126%
4	Fixed carbon	83.469%
5	BET surface area ($m^2 gm^{-1}$)	405.0
6	Micro-pore volume	0.2856 $cm^3 gm^{-1}$
7	Point of zero charge	8.6

Fig. 1. Before (a) and after (b) RH adsorption, the surfaces of activated charcoal 50× magnification.

3.2. Effect of adsorbent dose

The quantity of the adsorbent is a crucial parameter for the sorption capacity of adsorbent in a given operating condition. Adsorbent doses varying from 0.075 g to 1 gm per liter were used in this study as shown in Fig. 2. In the dosage range of 0–0.2 g, the removal efficiency of RH increased sharply; when the dosage was beyond 0.2 g, the RH removal rate was almost the same, only slightly decreased when the dosage was beyond 0.75 g. More removal of RH by the adsorbent is due to the fact that higher the adsorbent dose, higher the adsorbent mass and adsorbent area, higher is the active sorption site and adsorption [49]. The decrease in the removal of RH is due to the

saturation of the active site of adsorbent by almost all RH molecules and reversal of desorption. The optimum value of adsorbent was found to be 0.75 g L^{-1} and was used for the rest of the study.

3.3. Effect of solution pH

The effect of pH on adsorption of RH was studied over activated carbon from MH in the pH range of 2–10 (Fig. 3). In this study, the pH was adjusted using 0.1 (N) HCl or 0.1 (N) NaOH. The effect of pH in RH can be explained by considering the surface charge of activated carbon (pH$_{pzc}$) and dissociation constant (pK_a) of RH. The point of zero charge (pH$_{pzc}$) is the
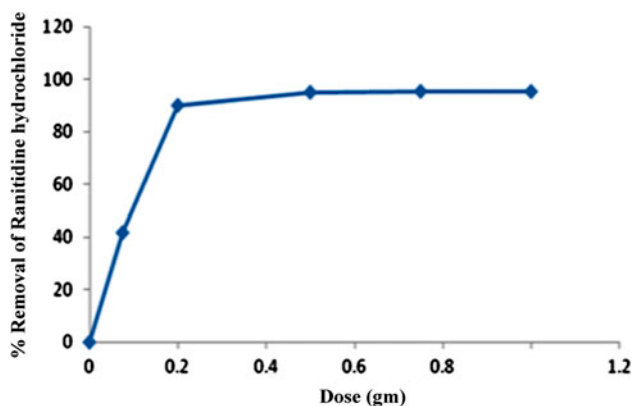

Fig. 2. Effect of adsorbent dose on the adsorption of RH by AC-MBH (experimental conditions: initial drug concentration: 100 mg L^{-1}, pH 7, agitation speed: 120, temperature: 298 K).
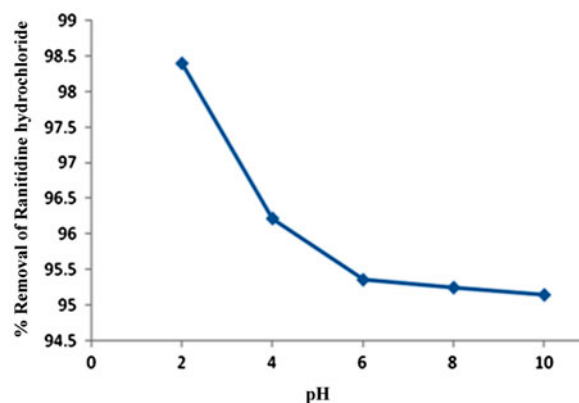

Fig. 3. Effect of pH on the adsorption of RH by AC-MBH (experimental conditions: initial drug concentration: 100 mg L^{-1}, dose: 0.75 gm, agitation speed: 120, temperature: 298 K).

zero electrical charge density on the surface of an adsorbent at a certain pH. The pHpzc of the activated carbon was experimentally found to be 8.6. When the pH < pH$_{pzc}$, the adsorbent surface becomes positively charged so it attracts negatively charged particle (anion) where it repels positively charged cationic particle. The dissociation constant (pK_a) of RH is 8.2 and 2.7; it signifies that at a value of 2.7, it is highly protonated, whereas in case of value 8.2, it is weakly protonated. Therefore, in case of pH 2, the activated carbon surface becomes positive (pH < pH$_{pzc}$) where the drug becomes highly protonated (pH < pK_a) so adsorptive removal occurs more as compared to pH 8.2, where the drug molecule weakly protonated. Therefore, the electrostatic interactions play the major role in the RH adsorption on activated carbon. From Fig. 3, it was shown that at pH 2, maximum removal of RH was occurred, while at pH 10, removal of RH was minimum. Similar types of trends were found in the case of other carbon compounds for the removal of PCs [27,50].

3.4. Effect of agitation

One of the most important factors influencing the adsorption kinetics is the agitation speed. The sorption study was done by varying the agitation speed from 40 to 240 rpm. From Fig. 4, it is seen that increasing agitation speed from 40 to 180 rpm resulting drug adsorption increased from 90.48 to 99.1%. The curve behavior can be explained by the fact that at low agitation speed (80 rpm), the spreading of the sample was not done properly and samples were accumulated; thus, only the upper layer was available for adsorption so removal rate is somewhat low.
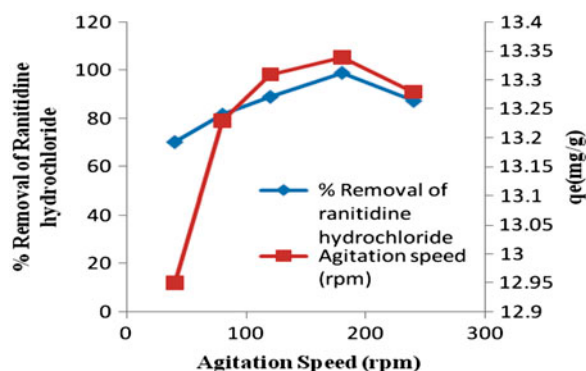

Fig. 4. Effect of agitation speed on the adsorption of RH by AC-MBH (experimental conditions: initial drug concentration: 100 mg L^{-1}, dose: 0.75 gm, pH 2, temperature: 298 K).

Increasing the agitation speed (from 40 to 180 rpm) increases the rate of diffusion of RH molecules from the bulk liquid to the liquid boundary layer surrounding the particle due to increase of both turbulence and external film transfer coefficient, whereas decrease of the thickness of the liquid boundary layer resulting increases adsorption. The lowering of RH removal happened after a further increase of speed (180 rpm) due to desorption of the compound due to strong centrifugal force. The best agitation speed was thus found to be 180 rpm and this speed had been taken for the rest of the study.

3.5. Optimization of RH removal using the RSM

According to the CCD matrix in Table 4, the experiment was designed and results were obtained. An empirical relationship between the response and the three independent variables has been expressed in quadratic model equation in terms of coded variables given in Eq. (4) and in terms of actual variables in Eq. (5).

$$\% \text{ Removal of RH} = 97.50 + 9.93 \times A + 0.077 \times B - 2.17 \times C - 2.04 \times A \times B + 2.53 \times A \times C - 0.25 \times B \times C - 8.42 \times A^2 + 0.22 \times B^2 - 1.87 \times C^2 \tag{4}$$

$$\% \text{ Removal of RH} = R1 = 45.14264 + 0.099284 \times \text{dose} + 1.17835 \times \text{pH} + 0.068049 \times \text{rpm} - 1.70312E{-}003 \times \text{dose} \times \text{pH} + 1.26375E{-}004 \times \text{dose} \times \text{rpm} - 1.67333E{-}003 \times \text{pH} \times \text{rpm} - 5.26519E{-}005 \times \text{dose}^2 + 0.024453 \times \text{pH}^2 - 7.48051E{-}004 \times \text{rpm}^2 \tag{5}$$

Results obtained for second-order response surface model in the form of analysis of variance (ANOVA) are shown in Table 5. ANOVA is used to check the statistical significance of the quadratic model. The fishers F-value (204.43) along with the very low probability value (<0.0001) suggest the regression model was highly significant. Multiple correlation coefficient (R^2) between the experimental and the model predicted values of the response variable was also assessed to check the goodness of fit of the model. In this experiment, a fairly high R^2 value of 0.9946 revealed that the model was statistically significant and only 0.54% of the total variance was not explained by the model.

Table 4
CCD for three independent process variables along with the observed response

Run no.	Coded values			Real values			Percent removal of RH
	A	B	C	A	B	C	
	0	0	$-\alpha$	750.00	7.00	45.91	95.54
	0	0	0	750.00	7.00	130.00	97.86
	+1	+1	−1	1,150.00	10.00	80.00	96.044
	0	0	0	750.00	7.00	130.00	98.84
	0	0	0	750.00	7.00	130.00	98.9
	−1	+1	−1	350.00	10.00	80.00	85.039
	−1	−1	+1	350.00	4.00	180.00	70.02
	0	0	0	750.00	7.00	130.00	96.79
	$+\alpha$	0	0	1,422.72	7.00	130.00	90.43
	0	0	0	750.00	7.00	130.00	96.78
	0	$+\alpha$	0	750.00	12.05	130.00	97.12
	0	$-\alpha$	0	750.00	1.95	130.00	99.32
	+1	−1	−1	1,150.00	4.00	80.00	98.17
	$-\alpha$	0	0	77.28	7.00	130.00	57.11
	−1	+1	+1	350.00	10.00	180.00	75.065
	−1	−1	−1	350.00	4.00	80.00	79.53
	+1	−1	+1	1,150.00	4.00	180.00	99.31
	0	0	0	750.00	7.00	130.00	95.78
	0	0	$+\alpha$	750.00	7.00	214.09	89.076
	+1	+1	+1	1,150.00	10.00	180.00	95.64

Table 5
ANOVA for the response surface quadratic model for RH removal

Sourc	Sum of squares	Degree of freedom (df)	Mean square	F-value	Prob. > F
Model	2,552.39	9	283.60	204.43	<0.0001
Residual	13.87	10	1.39		
Lack of fit	6.01	5	1.20	0.76	0.6127
Pure error	7.87	5	1.57		
Total	2,566.26	19			

Model statistics					
Standard deviation	Mean	C.V. (%)	R^2	Adjusted R^2	Predicted R^2
1.18	90.62	1.30	0.9946	0.9897	0.9777

The predicted multiple correlation coefficient value (0.9777) was in a reasonable good agreement with the adjusted multiple correlation value (0.9897) to confirm the significance of the model. Furthermore, the lack of fit value (>.05) showed the validity of the quadratic model in this study. A low value (1.30) of coefficient of variance suggests precision and reliability of the data.

From Table 6, it is observed that the coefficients of the main, square as well as interaction effects of the A (dose) and C (rpm) are highly significant ($p < 0.0001$) as compared to the other coefficient C (pH).

3.5.1. Effect of adsorbent dose and initial solution pH

The combined effect of adsorbent dose and initial solution pH on removal of RH can be predicted from the contour plot as shown in Fig. 5. It is observed that the % removal of RH was increased with increasing amount of adsorbent dose. This characteristic can be explained by the fact that increased adsorbent dose means a more adsorbent surface area thus more sorption site. The adsorbed RH amount decreases with increase of solution pH. This phenomena can be explained by the fact that when pH > pH_{pzc} (2.7 and

Table 6
Regression analysis using the 2^3 factorial CCD

Model term	Coefficient estimate	Standard error	F-value	p-value
A	9.93	0.32	969.77	<0.0001
B	0.077	0.32	0.059	0.812
C	−2.17	0.32	46.31	0.0001
AB	−2.04	0.42	24.09	0.0006
AC	2.53	0.42	36.84	0.0001
BC	−0.25	0.42	0.36	0.5601
A^2	−8.42	0.31	737.24	<0.0001
B^2	0.22	0.31	0.50	0.4943
C^2	−1.87	0.31	36.33	0.0001

8.2), the adsorbent surface becomes negatively charged so it repels positively charged cationic particles (drug molecules), thus adsorption became less.

3.5.2. Effect of adsorbent dose and rpm

The effect of different level of adsorbent dose and rpm is shown in the contour plot of Fig. 6. It was confirmed from the figure that both the independent variables have a positive effect on the removal of RH. This means that increasing percentage removal of pharmaceutical can be obtained by simultaneous increase in adsorbent dose and rpm.

3.5.3. Effect of pH and rpm

Fig. 7 illustrated the contour plot of the interactive effects of the two independent variables, that is pH and rpm. The regression analysis using 2^3 factorial CCD indicates that the model term pH and rpm

combinedly was not significantly influencing the percentage removal of pharmaceutical compound. The collective p-value (0.5601) of these two factors greater than 0.1000 confirms the insignificant effect of these two parameters.

3.6. ANN training for the optimization of the RH removal model

ANN architectures are mostly feed-forward networks, which were mainly trained through an error back propagation algorithm using the input data. The input and output data of network training were obtained from RH adsorption experimentation and experimental design was planned through CCD. Input nodes of ANN represent independent variable (dose, pH, and rpm) where the output nodes give the dependent variables (the response or the removal of RH). The nonlinear transformations were done in the hidden layer and this layer was used for computational
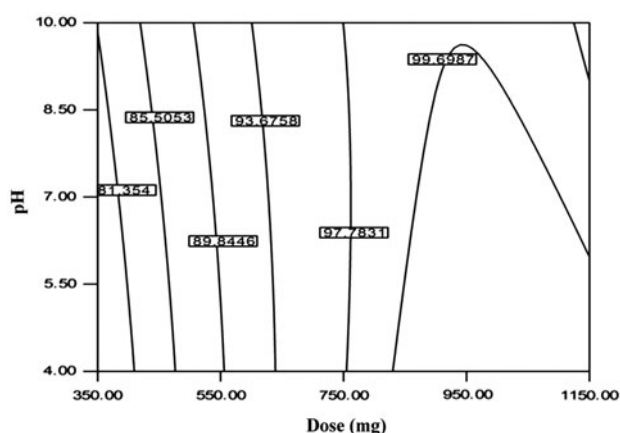

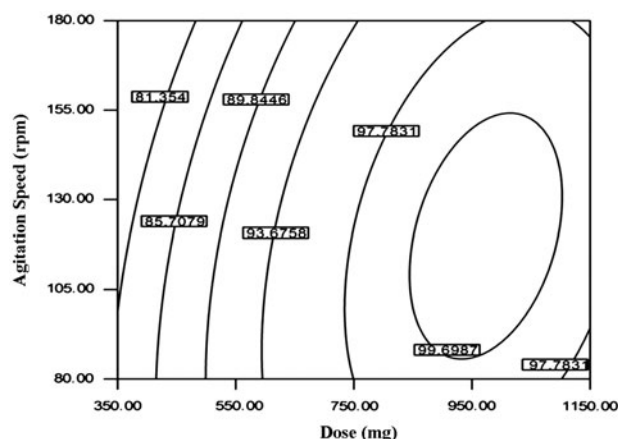Fig. 5. Contour plot showing effect of dose and pH on percent removal of RH.

Fig. 6. Contour plot showing effect of dose and agitation speed on percent removal of RH.
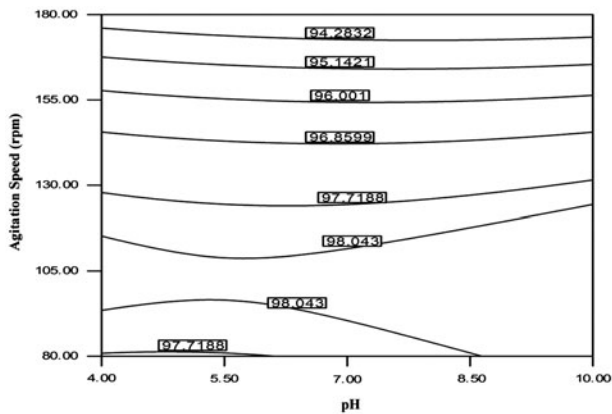
Fig. 7. Contour plot showing effect of pH and agitation speed.

purpose testing different types of algorithm for hidden layers, the best network was selected as one which gave coefficient of correlation (R^2) in close proximity to 1.

The optimization of ANN network is a crucial step for network training. POSLIN (a positive linear transfer function) and PURELIN were selected for the input and output mapping of hidden layer, respectively. The neurons within the hidden layer were optimized to give the best ANN network. The best correlation coefficient values were calculated after running the ANN software. The correlation coefficient was found

to be 0.99 from the regression plot of the trained network (Fig. 8). A high correlation coefficient that is closer to 1 signified the neural network modeling reliability with the experimental data. Table 7 showed that resilient backpropagation (Trainrp) algorithm was best suited for ANN networking as compared to other algorithms such as Levenberg–Marquardt backpropagation (Trainlm), conjugate gradient backpropagation with Polak–Ribiere updates (Traincgp), scaled conjugate gradient (Trainscg), and gradient descent with momentum and adaptive learning rate backpropagation (Traingdx).

3.7. Comparison of RSM and ANN network for the removal of RH

RSM and ANN modeling are used to solve linear and nonlinear multivariate regression problems. The comparative analysis of RSM and ANN was done by producing a difference of values of these two models as compared to the actual values. Validity of the two models was tested by conducting 10 new trials, consisting of a combination of experimental factors that does not belong to the training data-set. Table 8 shows the actual and predicted values along with the residuals for two models using 10 new trials. The distribution pattern of the residuals of two models, namely RSM and ANN is shown in Fig. 9. Residual
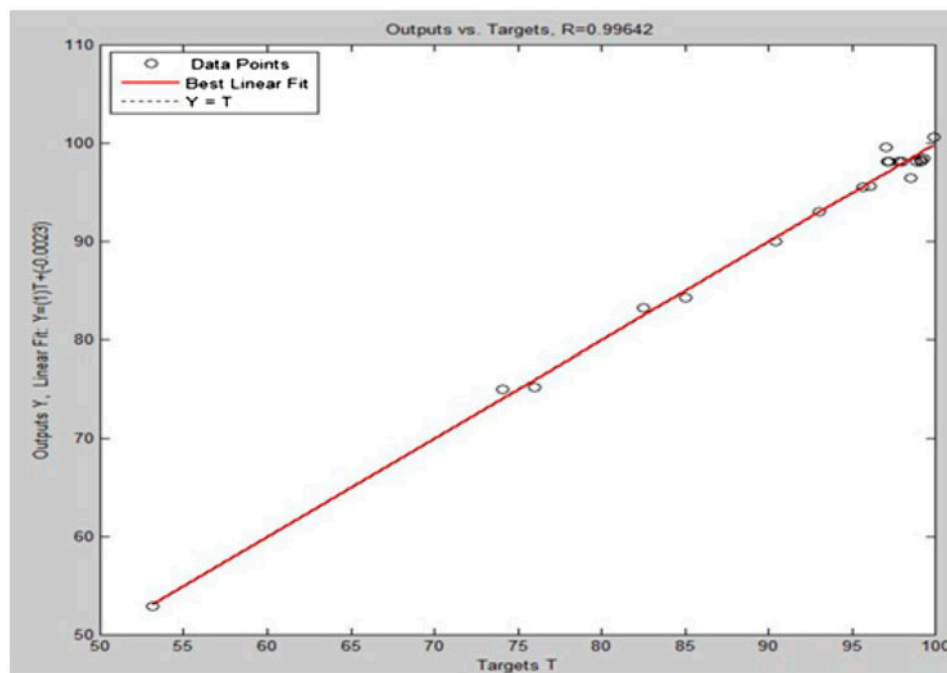

Fig. 8. Regression plot (actual vs. predicted) using three input variables, one output variable using ANN model.

Table 7
Trial and error method using transfer function (poslin and purelin) for % removal of RH by ANN model

Hidden layer algorithm	Output layer function	Correlation coefficient
Levenberg–Marquardt backpropagation	Trainlm	0.9635
Resilient backpropagation	Trainrp	0.9927
Scaled conjugate gradient backpropagation	Traincgp	0.9439
Conjugate gradient backpropagation with Polak–Ribiere updates	Trainscg	0.9579
Gradient descent with momentum and adaptive learning rate backpropagation	Traingdx	0.9512

Table 8
Validation data-set of RSM and ANN

Run	Dose (mg L^{-1})	pH	Agitation speed	% removal	RSM		ANN	
					Predicted	Residual	Predicted	Residual
1	550	3	180	95.23	94.43	0.792	96.29	−0.06
2	750	5	135	95.43	94.83	0.595	95.26	0.16
3	750	8.36	135	95.3	95.71	−0.412	95.53	−0.23
4	950	3	180	99.42	100.39	−0.97	99.25	0.16
5	950	7	90	96.34	95.23	1.104	96.22	0.11
6	750	5	59	88.92	86.62	2.296	88.86	0.059
7	550	7	180	95.32	95.47	−0.157	95.09	0.22
8	950	3	90	94.32	94.19	0.127	94.48	−0.16
9	550	3	90	88.2	88.23	−0.038	87.22	0.97
10	550	7	90	88.94	89.28	−0.34	88.97	−0.039

fluctuations of ANN are comparatively regular, small, and less deviation as compared to the RSM model. The performance of the models was estimated by three statistical estimators, namely RMSE, coefficient of determination (R^2), and AAD.

$$\text{RMSE} = \left(\frac{1}{n} \sum_{i=1}^{n} \left(T_{\% \text{ removal,predict}} - T_{\% \text{ removal,exp}} \right)^2 \right)^{1/2} \quad (6)$$

$$R^2 = \frac{\sum_{i=1}^{n} \left(T_{\% \text{ removal,exp}} - \overline{T_{\% \text{ removal,cal}}} \right)^2}{\sum_{i=1}^{n} \left(T_{\% \text{ removal,exp}} - \overline{T_{\% \text{ removal,cal}}} \right)^2 + \left(T_{\% \text{ removal,exp}} - T_{\% \text{ removal,cal}} \right)^2} \quad (7)$$

$$\text{AAD} = \left(\frac{1}{n} \sum_{i=1}^{n} \left(\frac{T_{\% \text{ removal,predict}} - T_{\% \text{ removal,exp}}}{T_{\% \text{ removal,exp}}} \right) \right) \times 100 \quad (8)$$

where n is the number of points, $T_{\% \text{ removal,predict}}$ is the predicted value, $T_{\% \text{ removal,exp}}$ is the actual value, and the symbol "−" is the average of the related values.

The statistical comparison of two models is presented in Table 9. A very good quality of predictions was done by both of these methods. ANN has some superior edge over RSM for fitting data as well as estimating capabilities. ANN approach is very flexible and does not require any standard experimental design to
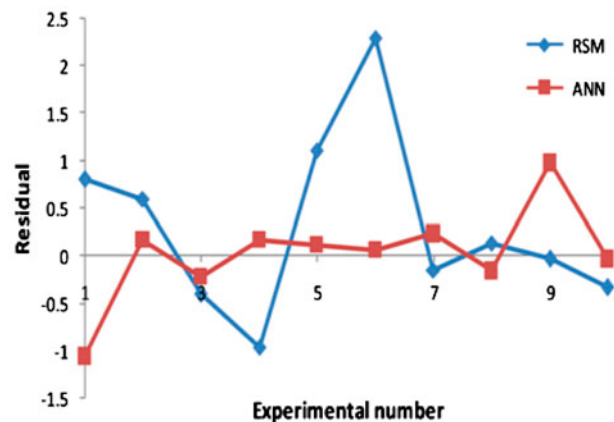

Fig. 9. Residuals distribution of RSM and ANN.

Table 9
Comparative statistical analysis of RSM and ANN

Parameters	RSM	ANN
RMSE	0.8740	0.2292
R^2	0.9357	0.9821
ADD (%)	0.3319	0.0271

build the model, but it does not give the effect of experimental factors and their interaction in comparison with RSM. Overall, the ANN approach would be more reliable, rational, and can develop and simulate process behavior as any form of nonlinearity and overcome quadratic nonlinear correlation assumption of RSM limitation.

4. Conclusion

The present investigation highlights the removal of RH from aqueous solutions employing superheated steam-activated carbon prepared from the abundantly available precursor material mung bean husk. Experimental study was done to find the influence of different process parameters (dose, pH, and agitation speed) on the removal process of ranitidine hydrochloride, and the optimized conditions were found to be best at agitation speed of 180 rpm, pH 2 and adsorbent dose of 0.75 gm l^{-1}. An attempt was made to model the removal process of RH using RSM and ANN. A design matrix was generated using CCD in RSM by selecting appropriate ranges of parameters. ANOVA study showed that of three process parameters viz adsorbent dose, agitation speed and combined effects of adsorbent dose and agitation speed were found to be significant to fit the experimental data. The removal process of RH over steam-activated carbon was efficiently predicted by constructing a three layer neural network along with ten neurons in the hidden layer. In the applied ANN model, the linear transfer function with resilient back propagation was found to be best fitted hidden layer algorithm. The effectiveness of the two models (RSM and ANN) was evaluated using residual fluctuations by validating the experimental results and statistically analyzed by RMSE, R^2, and AAD which indicated that ANN has some better predication capabilities as compared to RSM.

Acknowledgment

References

[1] T. Heberer, K. Reddersen, A. Mechlinskis, From municipal sewage to drinking water: Fate and removal of pharmaceutical residues in the aquatic environment in urban areas, Water Sci. Technol. 46 (2002) 81–88.

[2] M. Whelehan, U. von Stockar, I.W. Marison, Removal of pharmaceuticals from water: Using liquid-core microcapsules as a novel approach, Water Res. 44 (2010) 2314–2324.

[3] A. Kot-Wasik, J. Dębska, J. Namieśnik, Analytical techniques in studies of the environmental fate of pharmaceuticals and personal-care products, TrAC Trend. Anal. Chem. 26 (2007) 557–568.

[4] C.G. Daughton, T.A. Ternes, Pharmaceuticals and personal care products in the environment: Agents of subtle change? Environ. Health Perspect. 107 (1999) 907–938.

[5] D.W. Kolpin, E.T. Furlong, M.T. Meyer, E.M. Thurman, S.D. Zaugg, L.B. Barber, H.T. Buxton, Pharmaceuticals, hormones, and other organic wastewater contaminants in US streams, 1999−2000: A national reconnaissance, Environ. Sci. Technol. 36 (2002) 1202–1211.

[6] M. Petrović, M.D. Hernando, M.S. Díaz-Cruz, D. Barcelós, Liquid chromatography–tandem mass spectrometry for the analysis of pharmaceutical residues in environmental samples: A review, J. Chromatogar. A 2005 (1067) 1–14.

[7] N.A. Doerr-MacEwen, M.E. Haight, Expert stakeholders' views on the management of human pharmaceuticals in the environment, Environ. Manage. 38 (2006) 853–866.

[8] N. Vieno, T. Tuhkanen, L. Kronberg, Elimination of pharmaceuticals in sewage treatment plants in Finland, Water Res. 41 (2007) 1001–1012.

[9] R.L. Gomes, M.D. Scrimshaw, J.N. Lesters, Determination of endocrine disrupters in sewage treatment and receiving waters, TrAC Trends Anal. Chem. 22 (2003) 697–707.

[10] Z.-H. Liu, Y. Kanjo, S. Mizutani, Removal mechanisms for endocrine disrupting compounds (EDCs) in wastewater treatment—Physical means, biodegradation, and chemical advanced oxidation: A review, Sci. Total Environ. 407 (2009) 731–748.

[11] N. Nakada, T. Tanishima, H. Shinohara, K. Kiri, H. Takada, Pharmaceutical chemicals and endocrine disrupters in municipal wastewater in Tokyo and their removal during activated sludge treatment, Water Res. 40 (2006) 3297–3303.

[12] A. Gulkowska, H.W. Leung, M.K. So, S. Taniyasu, N. Yamashita, L.W. Yeung, B.J. Richardson, A. Lei, J.P. Giesy, P.K. Lam, Removal of antibiotics from wastewater by sewage treatment facilities in Hong Kong and Shenzhen, China, Water Res. 42 (2008) 395–403.

[13] Q. Sui, J. Huang, S. Deng, G. Yu, Q. Fan, Occurrence and removal of pharmaceuticals, caffeine and DEET in wastewater treatment plants of Beijing, China, Water Res. 44 (2010) 417–426.

[14] M. Isidori, A. Parrella, P. Pistillo, F. Temussi, Effects of ranitidine and its photoderivatives in the aquatic environment, Environ. Int. 35 (2009) 821–825.

[15] M.M. Huber, S. Canonica, G.-Y. Park, U. von Gunten, Oxidation of pharmaceuticals during ozonation and

advanced oxidation processes, Environ. Sci. Technol. 37 (2003) 1016–1024.

[16] R. Andreozzi, M. Canterino, R. Marotta, N. Paxeus, Antibiotic removal from wastewaters: The ozonation of amoxicillin, J. Hazard. Mater. 122 (2005) 243–250.

[17] R.F. Dantas, M. Canterino, R. Marotta, C. Sans, S. Esplugas, R. Andreozzi, Bezafibrate removal by means of ozonation: Primary intermediates, kinetics, and toxicity assessment, Water Res. 41 (2007) 2525–2532.

[18] J. Rivas, O. Gimeno, T. Borralho, J. Sagasti, UV-C and UV-C/peroxide elimination of selected pharmaceuticals in secondary effluents, Desalination 279 (2011) 115–120.

[19] A.M. Redding, F.S. Cannon, S.A. Snyder, B.J. Vanderford, A QSAR-like analysis of the adsorption of endocrine disrupting compounds, pharmaceuticals, and personal care products on modified activated carbons, Water Res. 43 (2009) 3849–3861.

[20] A. Mestre, J. Pires, J. Nogueira, A. Carvalho, Activated carbons for the adsorption of ibuprofen, Carbon 45 (2007) 1979–1988.

[21] L.A. Pérez-Estrada, S. Malato, W. Gernjak, A. Agüera, E.M. Thurman, I. Ferrer, A.R. Fernández-Alba, Photo-Fenton degradation of diclofenac: Identification of main intermediates and degradation pathway, Environ. Sci. Technol. 39 (2005) 8300–8306.

[22] G.R. Boyd, H. Reemtsma, D.A. Grimm, S. Mitra, Pharmaceuticals and personal care products (PPCPs) in surface and treated waters of Louisiana, USA and Ontario, Canada, Sci. Total Environ. 311 (2003) 135–149.

[23] J.H. Al-Rifai, H. Khabbaz, A.I. Schäfer, Removal of pharmaceuticals and endocrine disrupting compounds in a water recycling process using reverse osmosis systems, Sep. Purif. Technol. 77 (2011) 60–67.

[24] G.R. Boyd, S. Zhang, D.A. Grimm, Naproxen removal from water by chlorination and biofilm processes, Water Res. 39 (2005) 668–676.

[25] M. Ike, M. Asano, F. Belkada, S. Tsunoi, M. Tanaka, M. Fujitas, Degradation of biotansformation products of nonylphenol ethoxylates by ozonation and UV/TiO$_2$ treatment, Water Sci. Technol. 46 (2002) 127–132.

[26] R. Han, D. Ding, Y. Xu, W. Zou, Y. Wang, Y. Li, L. Zou, Use of rice husk for the adsorption of congo red from aqueous solution in column mode, Bioresour. Technol. 99 (2008) 2938–2946.

[27] R. Baccar, M. Sarrà, J. Bouzid, M. Feki, P. Blánquez, Removal of pharmaceutical compounds by activated carbon prepared from agricultural by-product, Chem. Eng. J. 211–212 (2012) 310–317.

[28] I. Cabrita, B. Ruiz, A. Mestre, I. Fonseca, A. Carvalho, C. Ania, Removal of an analgesic using activated carbons prepared from urban and industrial residues, Chem. Eng. J. 163 (2010) 249–255.

[29] Y. Yoon, P. Westerhoff, S.A. Snyder, M. Esparza, HPLC-fluorescence detection and adsorption of bisphenol A, 17β-estradiol, and 17α-ethynyl estradiol on powdered activated carbon, Water Res. 37 (2003) 3530–3537.

[30] S. Fukahori, T. Fujiwara, R. Ito, N. Funamizu, pH-Dependent adsorption of sulfa drugs on high silica zeolite: Modeling and kinetic study, Desalination 275 (2011) 237–242.

[31] L. Pasti, A. Martucci, M. Nassi, A. Cavazzini, A. Alberti, R. Bagatin, The role of water in DCE adsorption from aqueous solutions onto hydrophobic zeolites, Microporous Mesoporous Mater. 160 (2012) 182–193.

[32] B. Pan, D. Lin, H. Mashayekhi, B. Xing, Adsorption and hysteresis of bisphenol A and 17α-ethinyl estradiol on carbon nanomaterials, Environ. Sci. Technol. 42 (2008) 5480–5485.

[33] W.-T. Tsai, C.-W. Lai, T.-Y. Su, Adsorption of bisphenol-A from aqueous solution onto minerals and carbon adsorbents, J. Hazard. Mater. 134 (2006) 169–175.

[34] F. Cao, P. Bai, H. Li, Y. Ma, X. Deng, C. Zhao, Preparation of polyethersulfone–organophilic montmorillonite hybrid particles for the removal of bisphenol A, J. Hazard. Mater. 162 (2009) 791–798.

[35] C. Cheng, L. Ma, J. Ren, L. Li, G. Zhang, Q. Yang, C. Zhao, Preparation of polyethersulfone-modified sepiolite hybrid particles for the removal of environmental toxins, Chem. Eng. J. 171 (2011) 1132–1142.

[36] K. Shakir, H.F. Ghoneimy, A. Elkafrawy, S.G. Beheir, M. Refaat, Removal of catechol from aqueous solutions by adsorption onto organophilic-bentonite, J. Hazard. Mater. 150 (2008) 765–773.

[37] L.A. Shah, M.d.G. da Silva Valenzuela, A.M. Ehsan, F.R.V. Díaz, N.S. Khattaks, Characterization of Pakistani purified bentonite suitable for possible pharmaceutical application, Appl. Clay Sci. 83–84 (2013) 50–55.

[38] T.X. Bui, H. Choi, Adsorptive removal of selected pharmaceuticals by mesoporous silica SBA-15, J. Hazard. Mater. 168 (2009) 602–608.

[39] A.K. Jain, V.K. Gupta, S. Jain, A. Suhas, Removal of chlorophenols using industrial wastes, Environ. Sci. Technol. 38 (2004) 1195–1200.

[40] N. Tomooka, The Asian Vigna: Genus Vigna Subgenus Ceratotropis Genetic Resources, Springer Science & Business Media, The Netherlands, 2002.

[41] M.A. Bezerra, R.E. Santelli, E.P. Oliveira, L.S. Villar, L.A. Escaleira, Response surface methodology (RSM) as a tool for optimization in analytical chemistry, Talanta 76 (2008) 965–977.

[42] D.C. Montgomery, Design and Analysis of Experiments, John Wiley & Sons, North Carolina, 2008.

[43] R. Azargohar, A. Dalai, Production of activated carbon from Luscar char: Experimental and modeling studies, Microporous Mesoporous Mater. 85 (2005) 219–225.

[44] J.P. Maran, S. Manikandan, K. Thirugnanasamband-ham, C.V. Nivetha, R. Dinesh, Box–Behnken design based statistical modeling for ultrasound-assisted extraction of corn silk polysaccharide, Carbohydr. Polym. 92 (2013) 604–611.

[45] A. Khataee, A. Khanis, Modeling of nitrate adsorption on granular activated carbon (GAC) using artificial neural network (ANN), Int. J Chem. React. Eng. 7 (2009) A5.

[46] J. Garrido, A. Linares-Solano, J. Martin-Martinez, M. Molina-Sabio, F. Rodriguez-Reinoso, R. Torregrosa, Use of nitrogen vs. carbon dioxide in the characterization of activated carbons, Langmuir 3 (1987) 76–81.

[47] D. Mohan, A. Sarswat, V.K. Singh, M. Alexandre-Franco, C.U. Pittman Jr., Development of magnetic activated carbon from almond shells for trinitrophenol removal from water, Chem. Eng. J. 172 (2011) 1111–1125.

[48] S. Mondal, K. Sinha, K. Aikat, G. Halder, Adsorption thermodynamics and kinetics of ranitidine hydrochloride onto superheated steam activated carbon derived from mung bean husk, J. Environ. Chem. Eng. 3 (2015) 187–195.

[49] M. Ghaedi, A. Ansari, M. Habibi, A. Asghari, Removal of malachite green from aqueous solution by zinc oxide nanoparticle loaded on activated carbon: Kinetics and isotherm study, J. Ind. Eng. Chem. 20 (2014) 17–28.

[50] S.K. Behera, S.-Y. Oh, H.-S. Park, Sorption of triclosan onto activated carbon, kaolinite and montmorillonite: Effects of pH, ionic strength, and humic acid, J. Hazard. Mater. 179 (2010) 684–691.